Journal of Radiation Research, Vol. 57, No. 5, 2016, pp. 499–504
doi: 10.1093/jrr/rrw053
Advance Access Publication: 5 July 2016

Consecutive CT-guided core needle tissue biopsy of lung lesions in the same dog at different phases of radiation-induced lung injury

Zhongyuan Yin, Sisi Deng, Zhiwen Liang and Qiong Wang*

Cancer Center, Union Hospital, Tongji Medical College, Huazhong University of Science and Technology, 1277 JieFang Avenue, Wuhan 430022, China
*Corresponding author. Cancer Center, Union Hospital, Tongji Medical College, Huazhong University of Science and Technology, 1277 JieFang Avenue, Wuhan 430022, China. Tel: +86-159-2739-5672; Fax: +86-27-6565-0733; Email: wdyxywq@163.com
Received December 26, 2015; Revised March 16, 2016; Accepted April 3, 2016

ABSTRACT

This project aimed to set up a Beagle dog model of radiation-induced lung injury in order to supply fresh lung tissue samples in the different injury phases for gene and protein research. Three dogs received 18 Gy X-ray irradiation in one fraction, another three dogs received 8 Gy in each of three fractions at weekly intervals, and one control dog was not irradiated. Acute pneumonitis was observed during the first 3 months after radiation, and chronic lung fibrosis was found during the next 4–12 months in all the dogs exposed to radiation. CT-guided core needle lung lesion biopsies were extracted from each dog five times over the course of 1 year. The dogs remained healthy after each biopsy, and 50–100 mg fresh lung lesion tissues were collected in each operation. The incidence of pneumothorax and hemoptysis was 20% and 2.8%, respectively, in the 35 tissue biopsies. A successful and stable radiation-induced lung injury dog model was established. Lung lesion tissue samples from dogs in acute stage, recovery stage and fibrosis stage were found to be sufficient to support cytology, genomics and proteomics research. This model safely supplied fresh tissue samples that would allow future researchers to more easily explore and develop treatments for radiation-induced lung injury.

KEYWORDS: radiation-induced lung injury, biopsy, animal model, normal tissue

INTRODUCTION

Several studies have shown that increasing the radiation dose in malignant thoracic tumors such as non–small cell lung cancer and lymphoma can result in better local control [1]. However, dose escalation can lead to radiation-induced lung injury, which is the most prevalent dose-limiting side effect in normal lung tissue. Typically, two distinct clinical, pathological and radiographic phases of radiation-induced lung injury have been recognized: an early phase of radiation pneumonitis (RP), which usually occurs between 1 and 6 months after radiation therapy, and a later phase of chronic radiation fibrosis, which usually occurs at between 6 and 12 months. In addition to other severe complications after radiotherapy, over 50% of patients suffer from lung injury [2]. Because this side effect is associated with high mortality, accurate prediction and comprehensive treatments following high-dose radiation are urgently needed. Unfortunately, no effective predictors of radiation exposure side effects or drugs approved by the Food and Drug Administration (FDA) are available to counteract its effects.

This may be caused by a lack of understanding of the mechanism of radiation-induced lung injury, which has three unique features, discussed as follows. (i) Lung injury occurs randomly. Although numerous studies have shown that the risk of inducing lung injury can be predicted by the mean lung dose (MLD) and the volume of lung receiving a dose greater than the threshold value (Vdose), such as V20 and V5 [3, 4] many patients with very low V20 still suffer from Grade III–IV RP in our clinic, suggesting that there may be genetic heterogeneity in the development of radiation-induced lung injury. (ii) Determining whether radiation-induced lung injury is a systemic reaction or a local response is challenging; a systemic reaction can be tracked by serum samples, while tissue samples, which can be difficult to obtain, are needed to track local development. (iii) Radiographic imaging of radiation-induced lung injury detected using a Computed

Tomography (CT) scan provides little information on the state of the radiated lung. Tissue samples provide more information on the molecular response of the lung tissue after radiation exposure. However, obtaining serial tissue samples throughout the entire process of RP is impossible. Thus, an animal model is needed to provide both blood and lung tissue samples during the development of radiation-induced lung injury.

The goals of this study were to develop a practical dog model to assess acute pneumonitis and chronic pulmonary fibrosis and to identify a method for obtaining injured lung tissue, whenever it is needed, from a living dog. In addition, we aimed to develop a model to examine the mechanism for and valuable predictors of radiation-induced lung injury for clinical use.

MATERIALS AND METHODS

Animals

We purchased and bred Beagle dogs from the Department of Veterinary Clinical Sciences of Tongji Medical College, Huazhong University of Science and Technology. At the time of purchase, they were 19–23 months old and weighed ~15 kg. All of the dogs underwent a physical examination. All studies were performed according to a protocol approved by the Huazhong University of Science and Technology Institutional Animal Care and Use Committee.

Radiation

To extract a biopsy sample of sufficient quantity, we used 18-gauge cutting core needles to extract lung lesion tissue from the dogs. The biopsy needles were obtained from Bard Biopsy System. The dogs were randomly assigned into three groups. Three dogs received 18 Gy X-ray (Priums-k, SIEMENS) radiation in one fraction. Another three dogs received 8 Gy in three fractions (at weekly intervals) for a total exposure of 24 Gy. One dog was never irradiated and was used as a control (Table 1). Approximately two-thirds of the right lung of each dog was exposed to radiation fields ranging from 7 × 14 to 8 × 17 cm. To protect the heart and spinal cord, we restricted 65–70% of the right lung volume, which was covered by a 95% prescription isodose line (Table 2).

CT scan

Weekly low dose CT scans of the dogs were performed at Week 4 after the first radiation exposure. The interval increased to 2 weeks from 4 weeks to 8 weeks, 4 weeks from 8 weeks to 24 weeks, and 8 weeks from 24 weeks to 40 weeks (Table 1). CT scans were performed using a third generation scanner (Siemens Balance) set at 0.5 cm slice thickness, 130 kVp and 90 mAs and a high resolution algorithm. The dogs were scanned in sternal recumbency 10 min after administration of pentobarbital sodium (Amersco, USA).

Biopsy

A surgical preparation was performed prior to the CT study, followed by an assessment of the location and selection of the target plane. The CT table was moved to the target plane, as indicated by the laser light in the gantry. In this plane, the site for needle insertion was subjectively chosen and marked. Subsequently, additional slices in the area of the marker were acquired to measure the distance from the skin to the proximal and distal borders of the biopsy area. The CT table was moved out of the gantry to insert the spinal needle. Full lung images were obtained to confirm complications. For each dog, this type of biopsy was performed once a week prior to the first exposure of radiation and 4, 8, 16 and 24 weeks after radiation exposure over the course of 1 year (Table 1).

Because healthy lung tissues are full of air, extracting intact and sufficiently healthy lung tissues using the regular CT-guided core needle biopsy is difficult, particularly in normal lung tissues, which tend to stick to the needle chamber. To overcome this obstacle, we injected 2–3 ml stroke-physiological saline solution into targeted healthy lung tissue using sterile syringes. The needle tip was withdrawn very slowly. A lung tissue volume of ~1.2 × 0.5 × 1.0 cm^3 would collapse (Fig. 1). The density of the collapsed lung tissues significantly increased, as shown by the CT scan images. This collapse allowed us to extract 25–30 mg of biopsy sample, as

Table 1. Schedule of CT scan surveillance, radiation and CT-guided needle biopsy for the seven dogs

		1 w-Pre	0 w	1 w	2 w	3 w	4 w	6 w	8 w	12 w	16 w	20 w	24 w	32 w	40 w
Control	Dog1	○■	○	○	○	○	○■	○	○■	○	○■	○	○■	○	○
24 Gy in three fractions	Dog2	○■	○◆	○◆	○◆	○	○■	○	○■	○	○■	○	○■	○	○
	Dog3	○■	○◆	○◆	○◆	○	○■	○	○■	○	○■	○	○■	○	○
	Dog4	○■	○◆	○◆	○◆	○	○■	○	○■	○	○■	○	○■	○	○
18 Gy in one fraction	Dog5	○■	○◆	○	○	○	○■	○	○■	○	○■	○	○■	○	○
	Dog6	○■	○◆	○	○	○	○■	○	○■	○	○■	○	○■	○	○
	Dog7	○■	○◆	○	○	○	○■	○	○■	○	○■	○	○■	○	○

CT = computed tomography, 8 Gy = X-Ray dose of 8 Gy, 18 Gy = X-Ray dose of 18 Gy, biopsy = CT-guided core needle lung biopsy. Dog 1, a control, did not receive any radiation; Dogs 2, 3 and 4 received 8 Gy radiation three times (at weekly intervals); and Dogs 5, 6 and 7 only received 18 Gy in a single acute exposure. All of the dogs were subjected to CT-guided lung core needle biopsy five times (at 1 week prior to the first radiation exposure and subsequently at 4, 8, 16 and 24 weeks after radiation). A weekly CT scan was performed on the dogs at 4 weeks after the first radiation exposure; the interval increased to 2 weeks from 4 weeks to 8 weeks, 4 weeks from 8 weeks to 24 weeks, and 8 weeks from 24 weeks to 40 weeks. W = week, open circle = CT Scan, closed diamond = radiation, closed square = biopsy.

Table 2. Actual and fractional volumes of right lung and heart irradiation

		Right lung volume (cm^3)	Fractional volume of right lung covered by 95% prescription isodose line (cm^3)/(%)	Fractional volume of right lung covered by 50% prescription isodose line (cm^3)/(%)	Heart volume (cm^3)	Fractional volume of heart covered by 95% prescription isodose line (cm^3)/(%)	Fractional volume of heart covered by 50% prescription isodose line (cm^3)/(%)
Control	Dog1	288			178		
24 Gy in three fractions	Dog2	280	190/68	258/92	173	3.46/2	27.7/16
	Dog3	285	185/65	262/92	177	3.54/2	33.6/19
	Dog4	278	195/70	264/95	175	5.25/3	29.8/17
18 Gy in one fraction	Dog5	275	179/65	254/92	178	5.34/3	30.3/17
	Dog6	280	196/70	260/93	173	3.46/2	34.6/20
	Dog7	290	194/67	267/92	175	5.25/3	28.0/16

To protect the heart and spinal cord, we restricted 65–70% of the right lung volume covered by 95% prescription isodose line and more than 90% volume covered by 50% prescription isodose line. Nevertheless, 2–3% of the heart was covered by 95% prescription isodose line, and less than 20% volume was covered by 50% prescription isodose line.

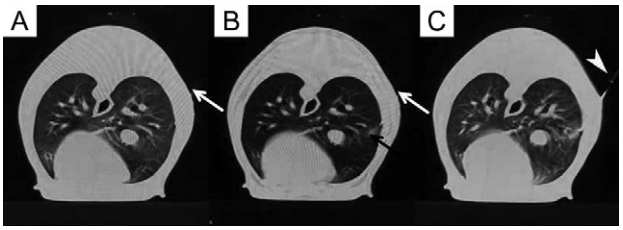

Fig. 1. CT images of healthy lung tissue biopsies. (A) Healthy lung before biopsy. (B) Lung image after injection of 2–3 ml stroke-physiological saline solution. (C) CT-guided biopsy. White arrow = syringe, black arrow = exudative area after injecting 2–3 ml stroke-physiological saline solution, white arrowhead = core needle.

opposed to traditional biopsies, which usually require only 10 mg of extracted tissue.

Record and sample collection

All of the animals were clinically monitored 24 h after each biopsy, depending on the clinical signs and severity of any complication. The weight, breath, body temperature, and appetite of the dogs were recorded throughout the next year. Lung tissues and blood serum from the dogs in various phases of the radiation response were used for hematoxylin–eosin (HE) staining, immunohistochemistry, and DNA and protein studies.

RESULTS

We recorded respiratory rates, body temperature, body weight, and appetite for all dogs. Only one dog (of six) in the 18 Gy X-ray group demonstrated an increased respiratory rate for 2 weeks. This symptom persisted for four weeks after receiving radiation and disappeared 2 weeks later. This dog did not show any other symptoms related to lung injury. The other five radiated dogs were similar to the control dog, and they remained alive and healthy throughout the entire experimental period of ~1 year.

A summary of CT appearances of RP and fibrosis for each subject is reported in Fig. 2. The area of the lesions grew, as detected using CT scans in the fourth, eighth, 16th and 24th weeks. The corresponding pathological examination after HE staining by a light microscope is also presented in this figure. Both groups presented similar CT images and pathological findings. No lung injury was observed in the control dogs. Figure 2A shows a CT image of the fourth week after irradiation, containing a large area of heterogeneous ground-glass opacity in the right lobe. The corresponding pathological examination was on the exudative stage, with a large amount of inflammatory cell infiltration in the alveolar cavity (Fig. 2AA). The CT image of the eighth week presented typical features of RP: ground-glass opacity and focal consolidation within the radiation portals, and a linear opacity in the right lung (Fig. 2B). The peculiarity of the pathology is that the alveolar space became smaller, the alveolar wall thickened and the number of fibroblasts increased. Concomitantly, alveolar Type II epithelial cells were hypertrophic, with the emergence of fibrin exudation. This stage was called the granulation growth period (Fig. 2BB). A well-defined consolidation in the right lower lobe, with associated parenchymal distortion, traction bronchiectasis, and lung volume loss was found on the CT image at the 16th week after radiation (Fig. 2C). The corresponding pathological stage was the period of fiber hyperplasia. A thickened alveolar wall with a reduced alveolar space was accompanied by an increase in fibers, fibroblasts and the number of Type II alveolar cells (Fig. 2CC). The last CT image of the 24th week depicts radiation fibrosis, with sharply marginated consolidation, dilatation and distortion of the lingular bronchus of the right lobe (Fig. 2D). This was

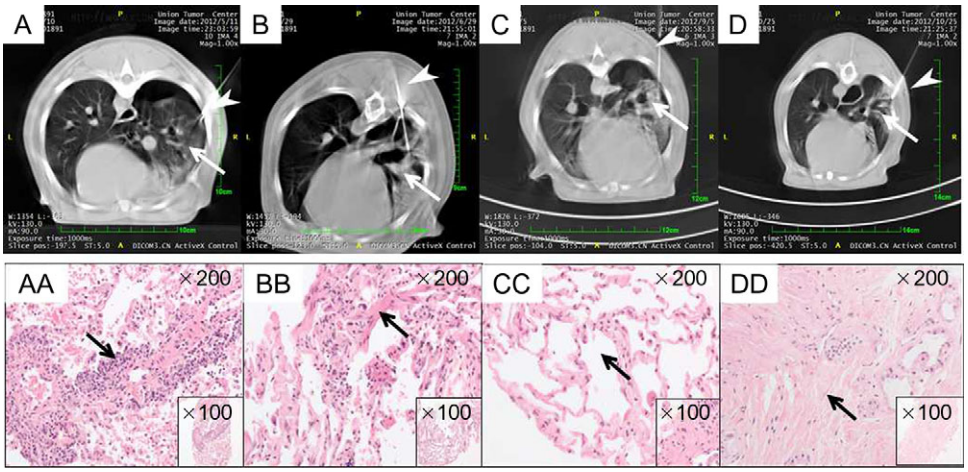

Fig. 2. CT images of core needle biopsies for injured lung lesions in different phases, and corresponding pathological changes in the same dog. (A) **Four weeks after radiation: a large area of heterogeneous ground-glass opacity in the right lobe (white arrow).** (B) **Eight weeks after radiation: typical features of radiation pneumonitis, including ground-glass opacity, focal consolidation within the radiation portals and a linear opacity (white arrow) in the right lung.** (C) **Sixteen weeks after radiation: a well-defined consolidation (white arrow) in the right lower lobe, with associated parenchymal distortion, traction bronchiectasis, and lung volume loss.** (D) **Twenty-four weeks after radiation: depiction of radiation fibrosis with sharply marginated consolidation, dilatation and distortion of the lingular bronchus of the right lobe (white arrow).** (AA) **Four weeks after radiation: exudative stage containing a large amount of inflammatory cell infiltration in the alveolar cavity (black arrow in AA).** (BB) **Eight weeks after radiation: granulation growth period, with a smaller alveolar space, a thicker alveolar wall and increased fibroblasts (black arrow in BB).** (CC) **Sixteen weeks after radiation: fiber hyperplasia period, with a thickened alveolar wall, clear alveolar reduction, increased fibers and fibroblasts, and increased numbers of Type II alveolar cells (black arrow in CC).** (DD) **Twenty-four weeks after radiation: collagen period, showing a local alveolar wall that was completely replaced by collagen tissue (black arrow in DD). The points of the core needles could be observed in lesions of the injured lung (arrowheads in A–D)**

the collagen period. The local alveolar wall was completely replaced with collagen tissue, and the pulmonary alveoli shrank and disappeared (Fig. 2DD). The pathological development over time was consistent with the change observed on CT scan images.

The percentages of pneumothorax and hemoptysis were 20% and 2.8%, respectively, for 35 biopsies (Table 3). Three out of seven dogs suffered from pneumothorax in the fourth week after radiation. In addition, one, one and two dog(s) suffered from pneumothorax in the eighth, 16th and 24th weeks, respectively. Only one dog coughed up blood when it received the core needle biopsy on the 24th week. This dog had successfully recovered after treatment with hemostasis medicine and penicillin for 5 days. We obtained 3–4 strips of the radiation-induced lesions or normal lung tissues for each biopsy. These strips weighed 25–30 mg, which was sufficient for HE staining, DNA extraction and protein studies.

Table 3. Incidences of pneumothorax and hemoptysis

		1 week-pre	4 weeks	8 weeks	16 weeks	24 weeks
Control	Dog1	○	○	○	○	○
24 Gy in three fractions	Dog2	○	●	○	○	○
	Dog3	○	○	○	○	●◆
	Dog4	○	●	○	○	○
18 Gy in one fraction	Dog5	○	○	○	○	●
	Dog6	○	○	●	●	○
	Dog7	○	●	○	○	○

No side effects. Pneumothorax (bullet). Haemoptysis (diamond). Three of the seven dogs suffered from pneumothorax on the fourth week after radiation. Furthermore, one, two and one dog(s) suffered from pneumothorax on the 8th, 16th and 24th week, respectively. Only one dog coughed up blood when it received core needle biopsy on the 24th week. The incidences of pneumothorax and hemoptysis were 20% and 2.8%, respectively.

DISCUSSION

In this study, we found that obtaining lung tissues multiple times is safe and convenient in Beagle dogs during the development of radiation-induced lung injury in both acute and chronic stages. Mice, rats, canines and rhesus macaques [5–8], have always been selected as experimental animal models for radiation-induced lung injury research. Mice and rats are small and easily manipulated with ionizing radiation exposure. However, for the same reason, these animals are too small to accurately expose the organ to radiation. For example, when the unilateral lung is established as the target organ, smaller animals always receive whole-body irradiation, which can elicit a general reaction on multiple organs rather than

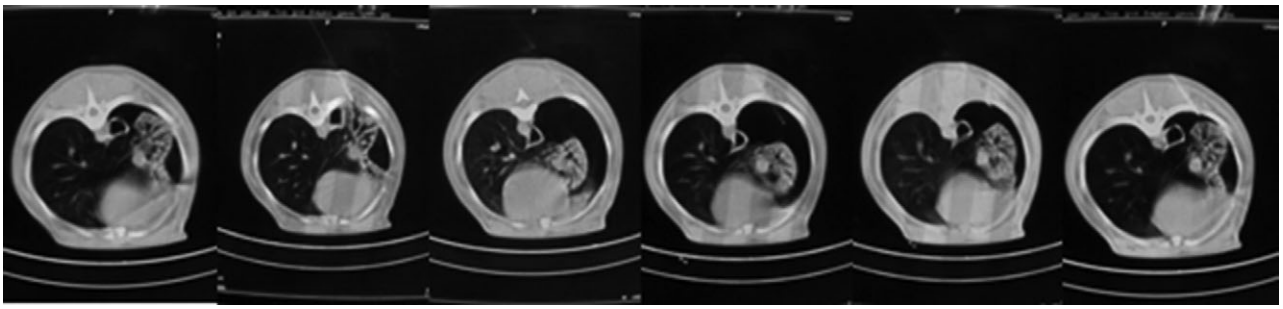

Fig. 3. CT images of pneumothorax. These six CT images show the right lung of a dog with pneumonitis that suffered from pneumothorax after receiving a core needle biopsy. Over half of the volume of the right lung had pneumothorax, which recovered soon after the air was sucked out six times using a 50 ml sterile syringe.

specifically on the lung tissue. Moreover, we cannot obtain lung tissues when these animals are alive. To obtain lung tissue from smaller animals, animals must be sacrificed during different stages of injury. One mouse or rat can provide corresponding lung tissue at one specific stage only. Thus, detecting a change in the tissues consecutively and dynamically in the same animal is difficult. Our results demonstrate that we can obtain injured lung tissue from the same Beagle dog multiple times using CT-guided core needle biopsy, which can provide sufficient samples for further cytological and histological evaluation. This may enable further exploration of the nature of radiation-induced lung injury. The same experiment can be performed on rhesus macaques; however, this procedure may be too expensive.

Only one of the six dogs exposed to radiation had an increased respiratory rate related to lung injury. This symptom cleared up without any treatment within 2 weeks. This dog did not show severe clinical symptoms such as intractable cough, dyspnea at rest, or the need for oxygen or steroid therapy. The other five radiated dogs were as healthy as the control dog, which may differ from patients undergoing thoracic radiotherapy. Inoue *et al.* [9] reported that 49% of patients exposed to definitive thoracic radiation experience clinical RP and that the RP is mild in 36% and severe in 13% of patients. The 3-year survival rates of the patients who have experienced no, mild and severe RP was reported as 33.4%, 38.2%, and 0%, respectively. Previous studies [10, 11] also showed that clinically significant RP usually develop in ~10% of patients. For animal research studies, Poulson *et al.* [6] showed that six (out of 37) dogs had severe symptomatic pneumonitis in 67% of the lung volume radiation group, and there was no morbidity related directly to lung toxicity in 33% of the lung volume radiation group. Our results are consistent with this study, but show dramatically lower RP rates compared with those of patients. The reasons for this may be as follows. (i) Better protection for non-targeted lung. Our CT image showed that the non-targeted lung was almost healthy, while patients with clinically severe RP always had lung injury based on CT images in both lungs. This is because more X-ray beams were applied in radiotherapy in clinical work to obtain the optimal dose distribution. (ii) Animal studies used a very low number of dogs for research compared with the large number of patients observed in clinical research. As such, the animal data require further verification.

Each dog received a core needle biopsy five times and a low-dose CT scan 13 times within 40 weeks. The CT appearance of RP in this canine model was similar to that observed in humans [12–14]. The pathological images of lung lesions at 0, 4, 8, 16 and 24 weeks after radiation show unique features. Exudative inflammation and granulation growth always occurred at the pneumonitis stage, while fibroplasia and collagenization were found in the fibrotic stage. Development of the CT scan and pathology images were consistent with each other in each dog. This could not be applied on patients or other animal models, which supported its use for gene and protein research.

Over the course of the 35 needle biopsies performed during the experiments, seven dogs suffered from pneumothorax seven times. This 20% occurrence rate was a little higher than that observed in clinical practice [15]. This may be related to the small lung volume of the Beagle dog. It is better to obtain tissues from the upper and middle lobes of the lung due to less breathing movement and vessel density in this area. The dogs had dyspnea and cyanosis of the tongue twice for ~1–2 min after the needle biopsy, suggesting a hypoxic condition. In addition, CT scans showed over half the volume of the unilateral lung pneumothorax. The lung recovered (Fig. 3) in 8–10 min after suction using a 50 ml sterile syringe. If the pneumothorax covered less than one-fifth of the volume of the unilateral lung and the dogs had no additional complications, then the biopsy could be safely continued without additional treatments.

Another side effect of the needle biopsy is pulmonary hemorrhage-induced hemoptysis, which can cause choking and suffocation. All of the dogs were anesthetized during the operations, and thus, their respiratory function was weakened. A reduction in choking risk requires prevention, not treatment. To avoid this risk, we avoided the part of the lung that was infused with wide-diameter blood vessels, particularly vessels with diameters >3 mm.

Almost all knowledge of carcinogenesis, development and treatment is dependent on both tumor cell and tissue research. In our clinical practice, we must offer the best support treatments to patients who develop radiation-induced lung injury. Obtaining injured lung tissues from patients to investigate the predictors, mechanisms and treatments of radiation-induced lung injury is impossible. Although multiple factors [16–19] have been reported to contribute to severe RP development in recent years, the progress has still been slow. No new drugs have been approved by the FDA for the treatment or prevention of RP, and the mortality rate in patients with severe RP is very high. Several important studies

[20] have already shown how to use Beagle dogs to establish a successful radiation-induced lung injury model. For the first time, we reported consecutive CT-guided core needle tissue biopsies of lung lesions in the same dog at different phases of radiation-induced lung injury. We recorded and bred this model for up to 1 year. None of the dogs were sacrificed or suffered from other diseases. This technique provides sufficient lung tissue and blood serum samples in the acute, recovery and fibrotic stages for further genomics, proteomics and cytological research studies. The technique can also effectively evade the genetic heterogeneity among animals that may confound discovery of the mechanism underlying lung injury. We propose that the present work is an important contribution to radiation-induced lung injury research.

ACKNOWLEDGEMENTS

We are grateful to Professor Gang Wu for taking overall responsibility for all aspects of the study, to the Department of Veterinary Clinical Sciences of Tongji Medical College, Huazhong University of Science and Technology for all their support, and to Benjamin Haley, who edited the manuscript.

FUNDING

This work was supported by The National Natural Science Funds from the National Natural Science Foundation of China [Grant number 81102074].

CONFLICT OF INTEREST

The authors declare that there are no conflicts of interest.

REFERENCES

1. Vogelius IR, Bentzen SM. A literature-based meta-analysis of clinical risk factors for development of radiation induced pneumonitis. *Acta Oncol* 2012;51:975–83.
2. Larici AR, del Ciello A, Maggi F, et al. Lung abnormalities at multimodality imaging after radiation therapy for non-small cell lung cancer. *Radiographics* 2011;31:771–89.
3. Vinogradskiy Y, Tucker SL, Liao Z, et al. A novel method to incorporate the spatial location of the lung dose distribution into predictive radiation pneumonitis modeling. *Int J Radiat Oncol Biol Phys* 2012;82:1549–55.
4. Yorke ED, Jackson A, Rosenzweig KE, et al. Dose–volume factors contributing to the incidence of radiation pneumonitis in non–small-cell lung cancer patients treated with three-dimensional conformal radiation therapy. *Int J Radiat Oncol Biol Phys* 2002;54:329–39.
5. Garofalo M, Bennett A, Farese AM, et al. The delayed pulmonary syndrome following acute high-dose irradiation: a rhesus macaque model. *Health Phys* 2014;106:56–72.
6. Poulson JM, Vujaskovic Z, Gillette SM, et al. Volume and dose–response effects for severe symptomatic pneumonitis after fractionated irradiation of canine lung. *Int J Radiat Biol* 2000;76:463–8.
7. Down JD, Medhora M, Jackson IL, et al. Do variations in mast cell hyperplasia account for differences in radiation-induced lung injury among different mouse strains, rats and nonhuman primates? *Radiat Res* 2013;180:216–21.
8. Du ZZ, Ren H, Song JF, et al. Rabbit model of radiation-induced lung injury. *Asian Pac J Trop Med* 2013;6:237–41.
9. Inoue A, Kunitoh H, Sekine I, et al. Radiation pneumonitis in lung cancer patients: a retrospective study of risk factors and the long-term prognosis. *Int J Radiat Oncol Biol Phys* 2001;49:649–55.
10. Abratt RP, Morgan GW. Lung toxicity following chest irradiation in patients with lung cancer. *Lung Cancer* 2002;35:103–9.
11. Ortholan C, Mornex F. Normal tissue tolerance to external beam radiation therapy: lung. *Cancer Radiother* 2010;14:312–8.
12. Trovo M, Linda A, El Naqa I, et al. Early and late lung radiographic injury following stereotactic body radiation therapy (SBRT). *Lung Cancer* 2010;69:77–85.
13. Bibault JE, Ceugnart L, Prevost B, et al. CT appearance of pulmonary carcinomas after stereotactic radiation therapy. *Diagn Interv Imaging* 2013;94:255–62.
14. Park KJ, Chung JY, Chun MS, et al. Radiation-induced lung disease and the impact of radiation methods on imaging features. *Radiographics* 2000;20:83–98.
15. Lee SM, Park CM, Lee KH, et al. C-arm cone-beam CT-guided percutaneous transthoracic needle biopsy of lung nodules: clinical experience in 1108 patients. *Radiology* 2013;271:291–300.
16. Tang C, Gomez DR, Wang H, et al. Association between white blood cell count following radiation therapy and radiation pneumonitis in non-small cell lung cancer. *Int J Radiat Oncol Biol Phys* 2014;88:319–25.
17. Mahmood J, Jelveh S, Zaidi A, et al. Targeting the renin–angiotensin system combined with an antioxidant is highly effective in mitigating radiation-induced lung damage. *Int J Radiat Oncol Biol Phys* 2014;89:722–28.
18. Castillo R, Pham N, Ansari S, et al. Pre-radiotherapy FDG PET predicts radiation pneumonitis in lung cancer. *Radiat Oncol* 2014;9:74.
19. Li H, Liu G, Xia L, et al. A polymorphism in the DNA repair domain of APEX1 is associated with the radiation-induced pneumonitis risk among lung cancer patients after radiotherapy. *Br J Radiol* 2014;87:20140093.
20. Forrest LJ, Mahler PA, Vail DM, et al. Computed tomographic evaluation of radiation pneumonitis in a canine model. *Radiat Oncol Investig* 1998;6:128–34.